

Establishment of dual priming oligonucleotide (DPO)-based real-time RT-PCR method for detecting infectious hematopoietic necrosis virus

Shihao Zheng^{a,1}, Jingwen Huang^{a,1}, Qiuji Li^a, Xinyue Zhou^a, Yutong Yang^a, Hongying Zhao^a, Wenlong Zhang^{a,b,*}, Yongsheng Cao^{a,*}

^a College of Veterinary Medicine, Northeast Agricultural University, Changjiang Street NO. 600, Harbin, China

^b Northeastern Science Inspection Station, China Ministry of Agriculture Key Laboratory of Animal Pathogen Biology, Harbin, China

ARTICLE INFO

Keywords:

Infectious hematopoietic necrosis virus
Dual priming oligonucleotide (DPO)
Real-time RT-PCR

ABSTRACT

Infectious hematopoietic necrosis virus (IHNV) is widely prevalent in the world, causing a large number of deaths in wild and farmed salmonids. Therefore, the establishment of an effective and accurate detection method is extremely important. In this study, the conservation of the N gene of IHNV was analyzed, followed by the design of dual priming oligonucleotide (DPO) for developing the real-time RT-PCR assay. The specificity and sensitivity of the method were analyzed and the results showed that only IHNV was positive and had high specificity in the detection of 8 aquatic animal viruses. The minimum detection limit was 3.62×10^1 copies/ μ L. Meanwhile, in the repeatability analysis, all CVs (coefficient of variation) were less than 1 %, indicating good repeatability. Notably, the presence of three or more base mismatches in the template significantly reduced amplification efficiency or even terminated the reaction completely. Furthermore, DPO primers allow a wider annealing temperature range, and the target gene can be successfully amplified in the annealing temperature range of 45 °C to 65 °C. Finally, the DPO-based real-time RT-PCR method could be used to detect the clinical samples with higher IHNV prevalence rate compared with the traditional RT-PCR. The IHNV detection approach utilizing DPO primers, as established in this study, showed excellent specificity and sensitivity, thus providing technical support for rapid and accurate identification of IHNV and facilitating the further multiplex real-time PCR establishment.

1. Introduction

Infectious hematopoietic necrosis (IHN) is a viral infection caused by infectious hematopoietic necrosis virus (IHNV), which predominantly infects salmonids (Kurath et al., 2016). IHNV is a single-stranded negative-sense RNA virus of the *Novirhabdovirus* genus within the *Rhabdoviridae* family (Walker et al., 2022). IHNV was first discovered in the United States in the 1950s (Rucker et al., 1953) and subsequently spread to Europe and Asia through horizontal and vertical transmission. At present, IHNV is globally distributed across multiple countries (Abbadi et al., 2021; Mulei et al., 2019). The mortality rate of fish infected with IHNV can reach up to 90 % (Williams et al., 1999). Due to the limits of clinical vaccines and effective therapeutic drugs, IHN has caused substantial economic losses to the global salmonid aquaculture industry and has become a major factor hindering the sustainable development of salmonid farming (Garver et al., 2013; Pan et al., 2024).

The diagnostic techniques for IHNV as recommended by the World Organisation for Animal Health (WOAH) include traditional virus detection methods like virus isolation and neutralization tests, which are time-consuming and laborious. Immunological detection methods such as enzyme-linked immunosorbent assay (ELISA) (Medina et al., 1992) and indirect immunofluorescence assay (IFA) (Arzen et al., 1991; Lapatra et al., 1989) have the advantages of being fast and high-throughput, but require specific antibodies, and there is difficulty in serum sampling from juvenile fish. At present, RT-PCR is a commonly used molecular biology method for detecting IHNV (Dhar et al., 2008). However, its application has high requirements for primers and often suffers from the problem of insufficient sensitivity.

Indeed, co-infections of IHNV with either IPNV or VHSV have been reported in many regions worldwide (Kolodziejek et al., 2008; Vilas et al., 1994). In China, co-infection of IHNV and IPNV was documented for the first time in 2019 (Xu et al., 2019b). In instances of co-infection

* Corresponding authors at: College of Veterinary Medicine, Northeast Agricultural University, No.600 Changjiang Road, Harbin, China.

E-mail addresses: zhangwenlong@neau.edu.cn (W. Zhang), caoy@neau.edu.cn (Y. Cao).

¹ The authors are contributed equally

Table 1
Primer sequence information.

Type of primers	Primer ID	Sequence(5' → 3')	Product sizes(bp)
Conventional primers	IHNV-N-F ^a	ATGACAAGCGCACTCAGAGAG	1176
	IHNV-N-R ^a	TCAGTGAATGAGTCGGAGTCT	
	IHNV-C-G1F ^b	CCGATCTCCACATCCCGAATAAATGACGTCTACGC	195
	IHNV-C-G1R ^b	CTTGGATACCTCGTCCACAGCGACCGTCATGCACATC	
	IHNV-C-G2F ^b	CAACAGGGTTCTTCGGGGGTCAGACGATAGAGAAGG	136
	IHNV-C-G2R ^b	GTGTACCATTGGCATCGGGGAGCTGGGAAGTACAGAG	
	IHNV-C-L1F ^b	CAGGCCGTGTGATGGCAGTCATCCTCAGAGTGCAC	100
	IHNV-C-L1R ^b	ATACCAATGGCTCCAGAGTTTCAGGAGGTCTATCGC	
	IHNV-C-N1F ^b	ACTGATGAGGATCGTAGCAGAGGCCCGGGGTAGCAGC	273
	IHNV-C-N1R ^b	CCCTCTCCGGTTGAGCCATCGCCATCGTACTTGGAG	
DPO primers	IHNV-C-N2F ^b	AGCGGGCGGTGAGTCATGTCGGAGGAGAGGGAA	195
	IHNV-C-N2R ^b	GCTTGTGTTGGGATCTGCGAAAAGTGGCGTCCAGTG	
	IHNV-DPO-NF ^c	AGCGGGCGGTGAGTCATGTCIIIIIIAGAGGGAA	195
	IHNV-DPO-NR ^c	GCTTGTGTTGGGATCTGCGAAIIIIICGTCCAGTG	
	IHNV-N-N3F ^d	AGCGGGCGGTGAGTCATGTCGGAGGATAGAGCA	195
IHNV-N-N3R ^d	GCTTGTGTTGGGATCTGCGAAAAGTGGCGCTGGTG		
Point mutation primers	IHNV-N-SN3F ^d	AGCGGGCGGTGCGTCAAGTAGGAGGAGAGGGAA	195
	IHNV-N-SN3R ^d	GCTTGTGTTAGGGTCTGCGAAAAGTGGCGTCCAGTG	
	IHNV-N-N5F ^d	AGCGGGCGGTGAGTCATGTCGGAGGCGGAGTCA	195
	IHNV-N-N5R ^d	GCTTGTGTTGGGATCTGCGAAAAGTGGAGCCTGGCG	
	IHNV-N-SN5F ^d	AGCGGGCTGTAAGCCAAGTAGGAGGAGAGGGAA	195
IHNV-N-SN5R ^d	GCTTGGTATCGGAGTCTGCGAAAAGTGGCGTCCAGTG	195	

“I” means deoxyinosine.

^a Primers were used for full-length amplification of the target gene to prepare standard plasmid.

^b Conventional primers for validity analysis.

^c DPO primers for the establishment of detection methods.

^d Primers for point mutation.

involving IHNV and other viruses, the clinical symptoms shown by the host may be caused by other viruses rather than the clinical characteristics of atypical IHNV. More specifically, when co-infection of IHNV and IPNV occurs, IHNV is able to promote IPNV proliferation (Shao et al., 2022a), while IPNV inhibits IHNV proliferation (Shao et al., 2022b). Co-infection of multiple viruses poses a serious challenge to the diagnosis and prevention of diseases.

Current diagnostic methods for IHNV, such as RT-PCR and virus isolation, are highly effective but may be hindered by the presence of inhibitors in complex tissue samples or the potential for cross-reactivity with other pathogens. This study aims to address these issues by developing a DPO primer-based RT-PCR approach. Compared with conventional primers, dual priming oligonucleotide (DPO) primers possess the characteristics of strong specificity, unique structure, and tolerance to a wide temperature range of annealing. The DPO primer was first proposed in 2007, which contains two independent specific regions (Chun et al., 2007). The 5'-segment can be stably paired with the target gene, and the 3'-segment is used to guide the specific extension of the PCR reaction. The two independent specific regions are connected by polydeoxyinosine (poly I) linker (Chamberlain et al., 1988). Any mismatch of three or more bases in either the 5' or 3' primer regions will prevent the PCR reaction. Recently, DPO primer has been widely utilized in multiplex PCR, real-time fluorescence PCR and other detection techniques with high primer requirements due to its characteristics and advantages (Carrara et al., 2013; Chung et al., 2014). Studies have shown that DPO primer can also perform high-specific amplification under non-optimal PCR conditions (Yeh et al., 2011). In addition, DPO primer can reduce the competitive effects between different primers during multiplex PCR, enabling simple and efficient detection with high specificity (See et al., 2021).

In this study, DPO primers were designed for the conserved region of IHNV, and an IHNV detection method based on DPO primers was established. It provided a simple, rapid and accurate detection method of IHNV, which laid a foundation for the subsequent generation of multiplex PCR detection of complex co-infections containing IHNV.

2. Materials and methods

2.1. Cells, virus and clinical specimens

Epithelioma Papulosum Cyprini (EPC) cells were cultured in M199 medium containing 10 % fetal bovine serum (Wisent, Canada) and 1 % penicillin-streptomycin solution (Biodragon, China) at 25 °C. IHNV DN23 was a clinical isolate and propagated in EPC cells at 15 °C (Huang et al., 2024). Clinical specimens including the liver, kidney and spleen tissues of rainbow trout were collected from several trout farms in China.

2.2. DPO design and validation

The genomic sequences of various IHNV strains were obtained from the NCBI database (<https://www.ncbi.nlm.nih.gov/>). The conservative analysis was carried out using the MegAlign (v7.1.0) in DNASTAR software. Finally, primers targeting the nucleoprotein (N), glycoprotein (G), and RNA-dependent RNA polymerase (L) genes were designed for further verification. Primer pairs were ordered from Comate Bioscience Co., Ltd., China. The details of primers are shown in Table 1.

Approximately 8 bases with GC contents greater than 40 % were selected as the 3'-segment, five deoxyinosines were used as poly (I) linker, and then approximately 20 bases were extended to the 5'-segment to ensure that the melting temperature (T_M) was greater than 65 °C. Conventional primers contain the same sequence as DPO primers, except for the poly (I) linker.

To obtain the cDNA of IHNV, EPC cells infected with IHNV were harvested for extraction of total RNAs using Trizol reagent (ABclonal Biotechnology Co., Ltd., China). Then, the cDNA was reverse transcribed based on the extracted RNAs by Maxima H Minus Reverse Transcriptase (Thermo Fisher Scientific, USA).

2.3. Plasmid standard

The full-length N gene of IHNV was amplified using primers IHNV-N-F/R with the prepared IHNV cDNA as the template in a laboratory thermal cycler (SensoQuest, Germany). The PCR system with a total

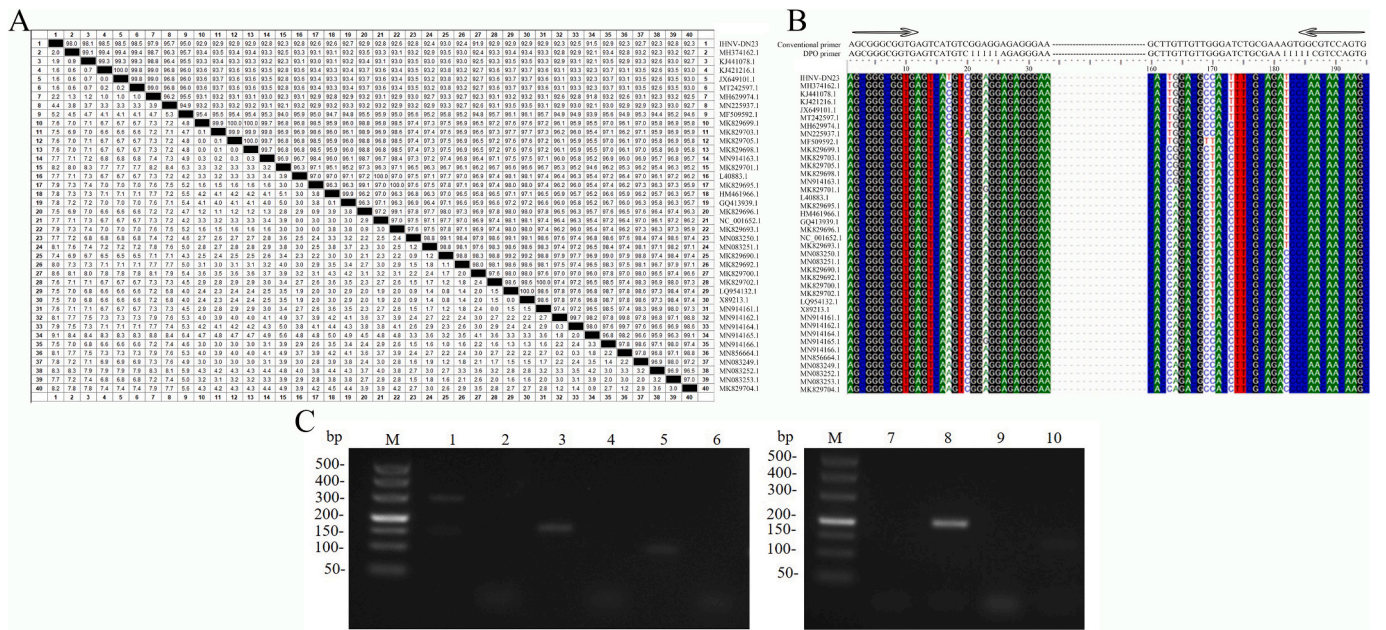


Fig. 1. Homology analysis of IHNV N gene nucleotide sequences and evaluation of primer effectiveness. A. Homology analysis of IHNV N gene nucleotide sequences. B. Schematic diagram of the binding regions of conventional primers and DPO primers across different IHNV strains. C. The experimental results of primer effectiveness. M, DL2000 DNA Marker; Lane 1, 3, 5, 8 and 10 were the amplification products using the paired primers of IHNV-C-N1F/R, IHNV-C-L1F/R, IHNV-C-G1F/R, IHNV-C-N2F/R and IHNV-C-G2F/R, respectively. Lane 2, 4, 6, 7 and 9 were the corresponding negative controls.

volume of 50 μ L was configured as follows: TransStart Fast Pfu PCR Super Mix (TransGen Biotech, Beijing, China) 25 μ L, cDNA 5 μ L, primer IHNV-N-F/R (10 μ M) 1 μ L, and ddH₂O 18 μ L. The reaction conditions were as follows: 95 $^{\circ}$ C for 2 min, followed by 30 cycles at 95 $^{\circ}$ C for 20 s, 52 $^{\circ}$ C for 20 s, 72 $^{\circ}$ C for 25 s, and finally at 72 $^{\circ}$ C for 5 min. The PCR product was ligated to the plasmid pEASY-Blunt (TransGen Biotech, Beijing, China) to obtain the recombinant plasmid pEASY-IHNV-N.

2.4. Evaluation of the specificity of DPO primers

As shown in Fig. 3, point mutations were introduced at the 3'- and 5'-binding sites of DPO primers using site-directed mutagenesis. Mutations at these positions were evaluated for their impact on primer-template binding efficiency and PCR amplification. The 5' or 3'-segments of the DPO primer binding sequence to the target gene had three site mutations (three site mutations occurred at the binding site of the 3'-segment of the reverse primer of DPO to the target gene, named FN3; three site mutations occurred at the binding site of the 3'-segment of the forward and reverse primers of DPO to the target gene, named N3; three site mutations occurred at the binding site of the 5'-segment of the forward and reverse primers of DPO to the target gene, named SN3) or five site mutations (five site mutations occurred at the binding site of the 3'-segment of the forward and reverse primers of DPO to the target gene, named N5; five site mutations occurred at the binding site of the 5'-segment of the forward and reverse primers of DPO to the target gene, named SN5). PCR was carried out using plasmid standard as a template, and the PCR system with a total volume of 50 μ L was as follows: TransStart Fast Pfu PCR Super Mix 25 μ L, plasmid pEASY-IHNV-N 1 μ L, primers (IHNV-C-N2F/IHNV-N-N3R, IHNV-N-N3F/R, IHNV-N-SN3F/R, IHNV-N-N5F/R, IHNV-N-SN5F/R) (10 μ M) 1 μ L, and ddH₂O 22 μ L. PCR amplification conditions were as follows: 95 $^{\circ}$ C for 2 min, followed by 30 cycles at 95 $^{\circ}$ C for 20 s, 52 $^{\circ}$ C for 20 s, 72 $^{\circ}$ C for 10 s, and 72 $^{\circ}$ C final extension of 5 min. Subsequently, the PCR product was ligated to the plasmid pEASY-Blunt to obtain the recombinant plasmids pEASY-N-FN3, pEASY-N-N3, pEASY-N-SN3, pEASY-N-N5, pEASY-N-SN5, respectively. Traditional PCR and real-time PCR were carried out with DPO primers IHNV-DPO-NF/R and conventional primers IHNV-C-N2F/R to

analyze the specificity of DPO primers.

2.5. Evaluation of the annealing temperature sensitivity of DPO primers

Traditional PCR was conducted using both DPO and conventional primers for comparison. The PCR annealing temperature was set within the range of 45 $^{\circ}$ C–65 $^{\circ}$ C to analyze the annealing temperature sensitivity of DPO primers.

2.6. Establishment of the standard curve

A standard curve was generated using SYBR Green qPCR Master Mix (ABP Biosciences) with five different concentrations of the standard plasmid, ranging from 3.62×10^8 to 3.62×10^4 copies/ μ L. Meanwhile, a negative control was established, and each dilution was tested in triplicate. The real-time PCR system with a total volume of 10 μ L was configured as follows: SYBR Green qPCR Master Mix 5 μ L, gradient diluted plasmid standards 1 μ L, primers IHNV-DPO-NF/R (10 μ M) 0.2 μ L, and ddH₂O 3.6 μ L. Real-time PCR was performed using the Light-Cycler 480 II instrument (Roche, Basel, Switzerland) under the following thermal cycling conditions: initial denaturation at 95 $^{\circ}$ C for 3 min; 40 cycles of 95 $^{\circ}$ C for 5 s, 60 $^{\circ}$ C for 30 s with fluorescence acquisition, and 95 $^{\circ}$ C for 5 s, 65 $^{\circ}$ C for 1 min; followed by a melting curve analysis with a ramp rate of 0.1 $^{\circ}$ C/s and continuous fluorescence acquisition up to 97 $^{\circ}$ C.

2.7. Specificity evaluation

The established detection method was used to assess specificity against IHNV, Snakehead vesiculovirus (SHVV) (Bei et al., 2023), Grass carp reovirus (GCRV) (Pei et al., 2014), Siniperca huatsi ranavirus (SCRaV) (Yu et al., 2023), Siniperca chuatsi rhabdovirus (SCRV), Carassius auratus herpesvirus (CaHV) (Ke et al., 2022), Andrias davidianus ranavirus (ADRV) and Rana grylio virus (RGV) (Ke et al., 2018). The total RNAs of IHNV, SHVV, GCRV and SCRv were extracted using Trizol, and were reverse transcribed into cDNA using Maxima H Minus Reverse Transcriptase. Meanwhile, the genomic DNA of ADRV, SCRaV, CaHV

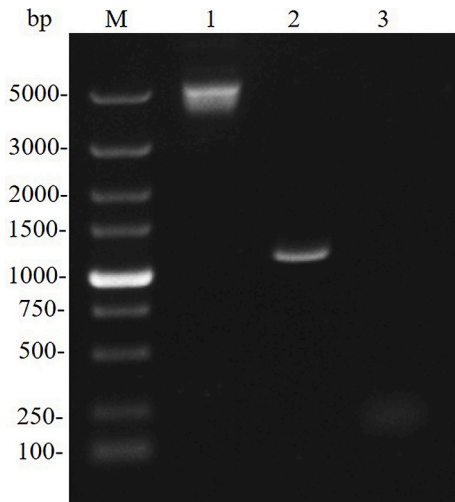


Fig. 2. PCR results based on the standard plasmid. M: DL2000 DNA Marker; 1: Standard plasmid; 2: Plasmid standard amplification product; 3: Negative control.

and RGV were extracted using TIANamp Virus DNA/RNA Kit, respectively (Tiagen Biotech, Beijing, China). Finally, the cDNAs and extracted genomic DNAs were used as templates for fluorescence quantitative PCR detection, with three replicates for each sample.

2.8. Evaluation of sensitivity and replicate consistency

The standard plasmid with a concentration of 3.62×10^{10} copies/ μL was diluted in a 10-fold gradient to a concentration ranging from 3.62×10^8 copies/ μL to 3.62×10^1 copies/ μL . The sensitivity of the method was analyzed by detecting plasmid DNA at different dilutions. In order to evaluate the repeatability of the method, we used a standard plasmid with concentrations of 3.62×10^8 copies/ μL , 3.62×10^6 copies/ μL , and 3.62×10^5 copies/ μL as templates. The average Ct value, standard deviation (SD) and coefficient of variation (CV) were calculated by using the established real-time PCR detection method for three intra-batch and inter-batch tests. Finally, the repeatability and stability of the method were analyzed according to the results of the CV calculation.

2.9. Sample testing

Finally, we collected 109 samples from several trout farms in China, consisting of *Salmo trutta*, *Oncorhynchus mykiss*, *Oncorhynchus masou*, *Brachymystax lenok*, and *Hucho taimen*. Total RNAs were extracted from a mixture of liver, spleen, and kidney tissues using Trizol, and then reverse transcription was carried out. Finally, these samples were detected using the method established in this study.

3. Results

3.1. Effectiveness analysis of primers

Nucleotide sequence comparison of the N gene of different strains of IHNV and effectiveness analysis of primers are shown in Fig. 1. The amplification efficiency of the IHNV-C-N2F/R primers was significantly higher than that of other primers. Therefore, we further optimized the IHNV-C-N2F/R primers by replacing specific nucleotide sequences (21–25 GGAGG in IHNV-C-N2F and 23–27 AGTGG in IHNV-C-N2R) with deoxyinosine to obtain IHNV-DPO-NF/R for the subsequent experiments.

3.2. Generation of the plasmid standard

The concentration of the recombinant plasmid was determined to be 200 ng/ μL by micro-spectrophotometer Nano-300 (ALLSHENG, China), and the copy number of the IHNV standard plasmid was calculated to be 3.62×10^{10} copies/ μL using the following formula: Copy number (copies/ μL) = (concentration(ng/ μL) $\times 10^{-9} \times 6.022 \times 10^{23}$) /DNA length $\times 660$. As shown in Fig. 2, a single-band product could be observed after the PCR amplification based on the plasmid standard.

3.3. DPO primer specificity analysis

As shown in Fig. 3, we used three or five base mutations designed within the 5' or 3'-segment of the N gene binding sequence of the DPO primers to evaluate the DPO primers' specificity using IHNV as a model. Traditional PCR (Fig. 4) and fluorescence quantitative PCR (Fig. 5) were carried out using DPO primers and conventional primers, respectively. The results showed that DPO primers had higher specificity than conventional primers. Notably, when there were more than three bases' mismatches between the template and the DPO primer, the PCR

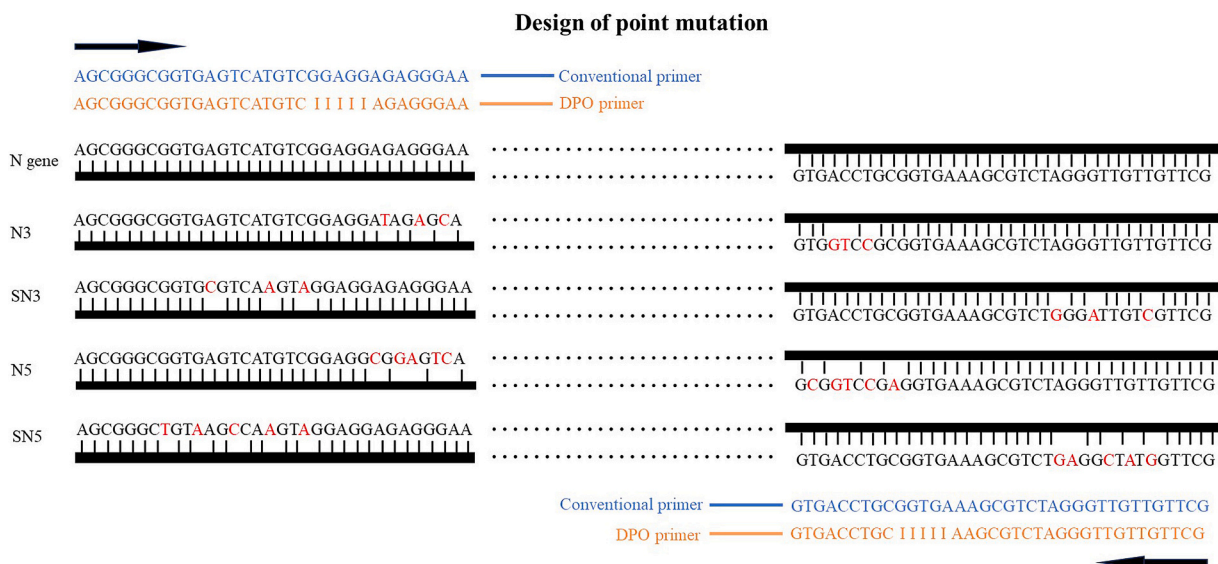


Fig. 3. Point mutation diagram.

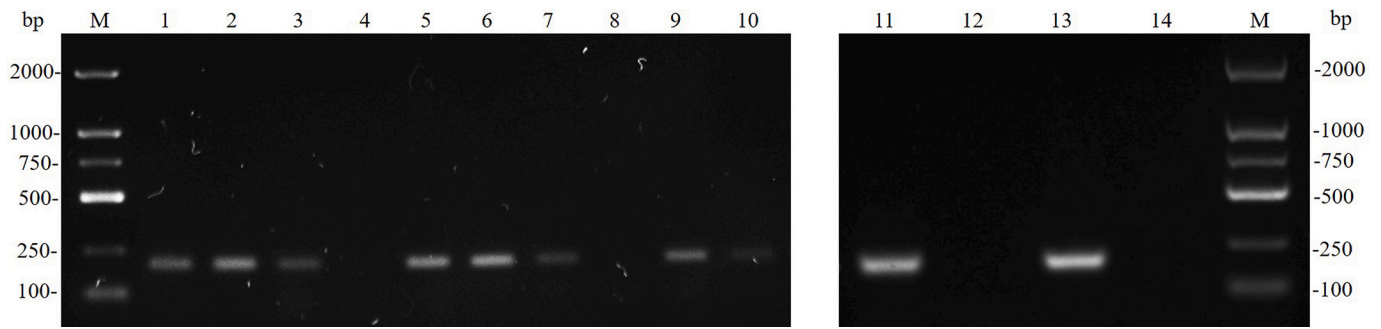


Fig. 4. Agarose gel electrophoresis results of traditional PCR amplification products based on conventional primers and DPO primers. M: DL2000 DNA Marker; 1: FN3 + conventional primers; 2: FN3 + DPO primers; 3: N3 + conventional primers; 4: N3 + DPO primers; 5: SN3 + conventional primers; 6: SN3 + DPO primers; 7: N5 + conventional primers; 8: N5 + DPO primers; 9: SN5 + conventional primers; 10: SN5 + DPO primers; 11: N gene + conventional primers; 12: Negative control for conventional primers; 13: N gene + DPO primers; 14: Negative control for DPO primers.

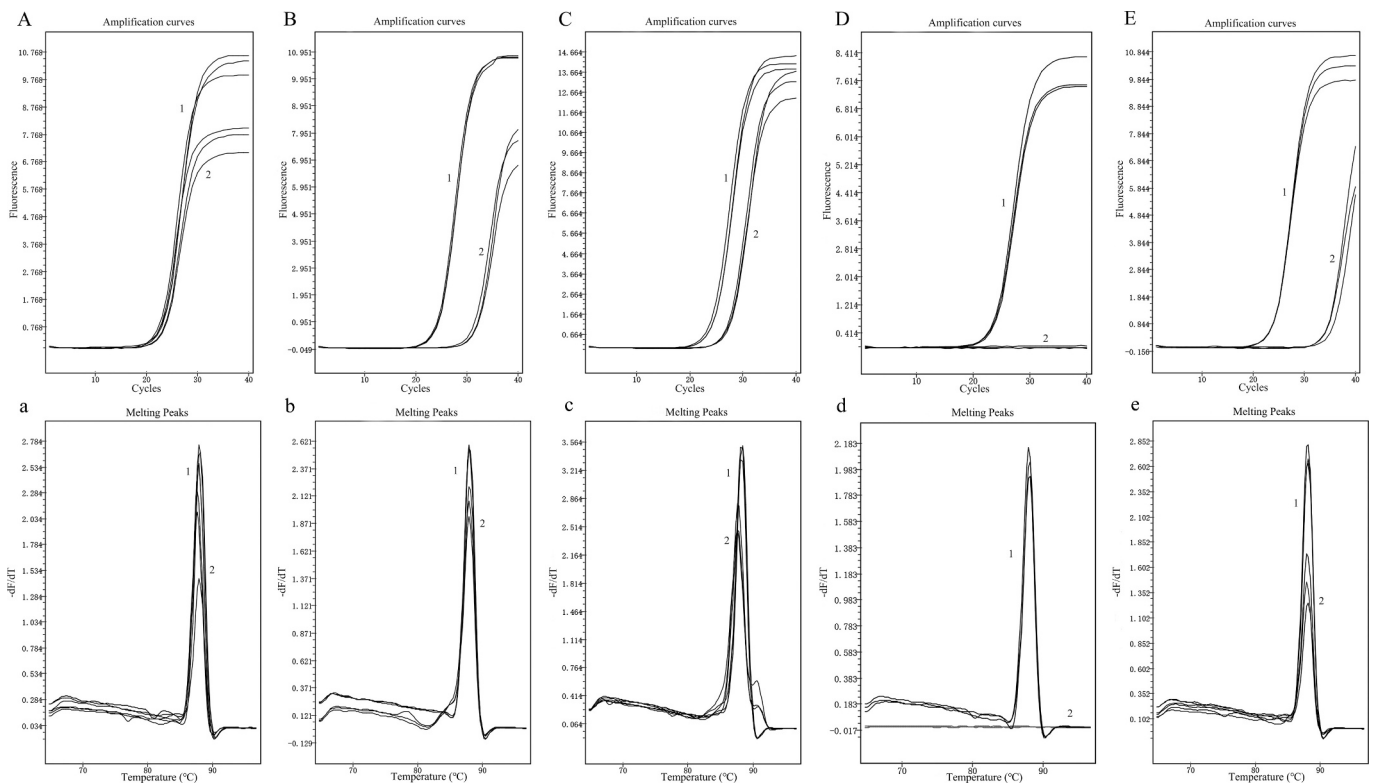


Fig. 5. SYBR Green fluorescence detection results based on conventional primers and DPO primers. A ~ E. Amplification curves. The templates were FN3, N3, SN3, N5 and SN5, respectively. a ~ e. The corresponding melting peaks. 1: Conventional primers + FN3/N3/SN3/N5/SN5, respectively. 2: DPO primers + FN3/N3/SN3/N5/SN5, respectively. (For interpretation of the references to colour in this figure legend, the reader is referred to the web version of this article.)

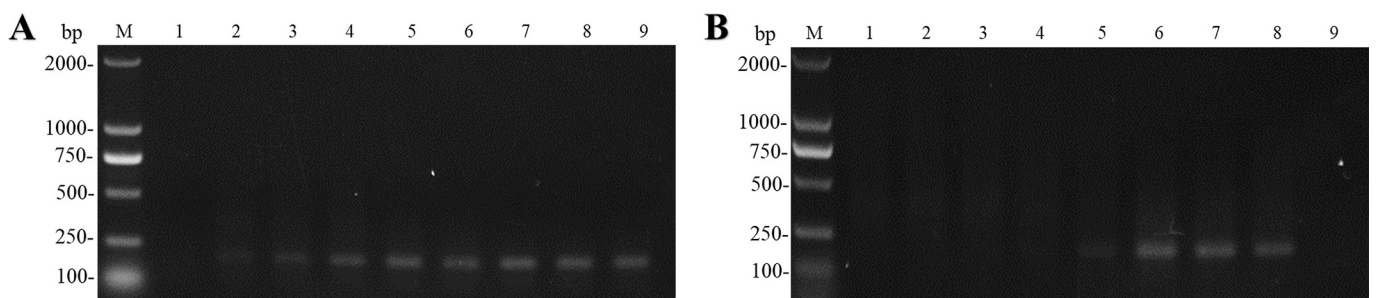


Fig. 6. Comparison of annealing temperature sensitivity between DPO primers and conventional primers. M: DL2000 DNA Marker. A. DPO primer amplification results. B. Conventional primer amplification results. 1: Negative control for DPO primers (Left), Negative control for conventional primers (Right). 2–9: Annealing temperature at 45 °C, 46.6 °C, 48.9 °C, 52.9 °C, 57.3 °C, 61.1 °C, 63.4 °C, 65 °C, respectively.

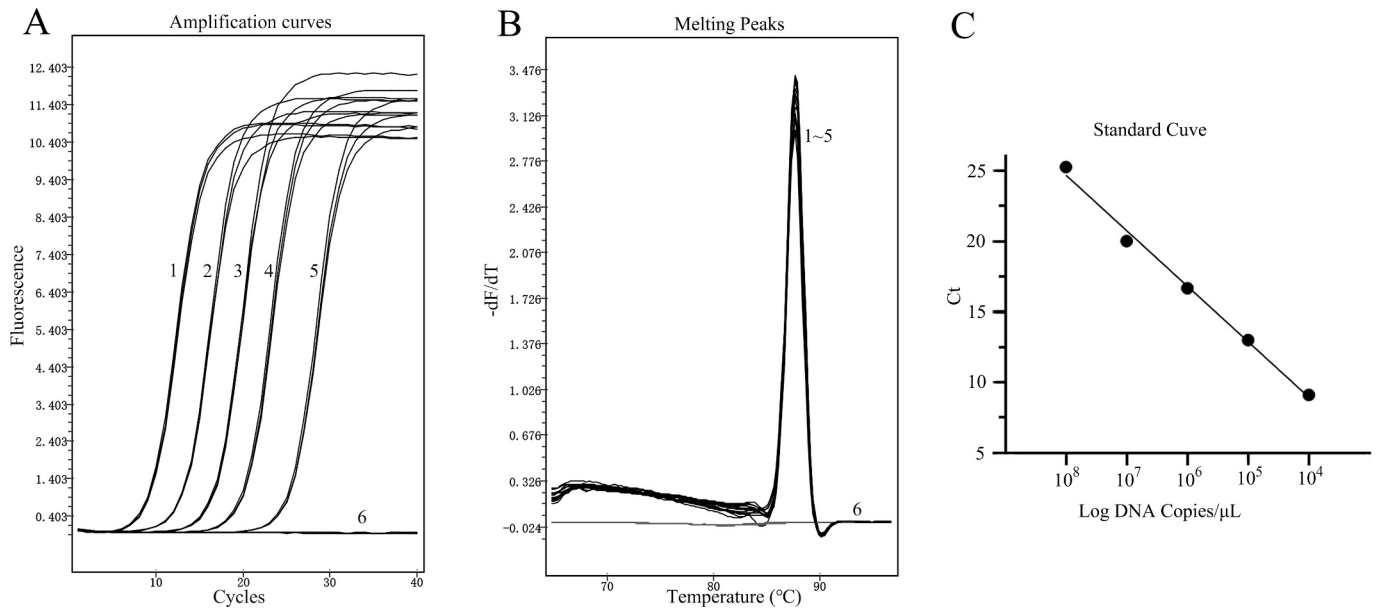


Fig. 7. The standard curve of DPO real-time PCR for IHNV. A. Amplification curves; B. Melting peaks; C. Standard curve.

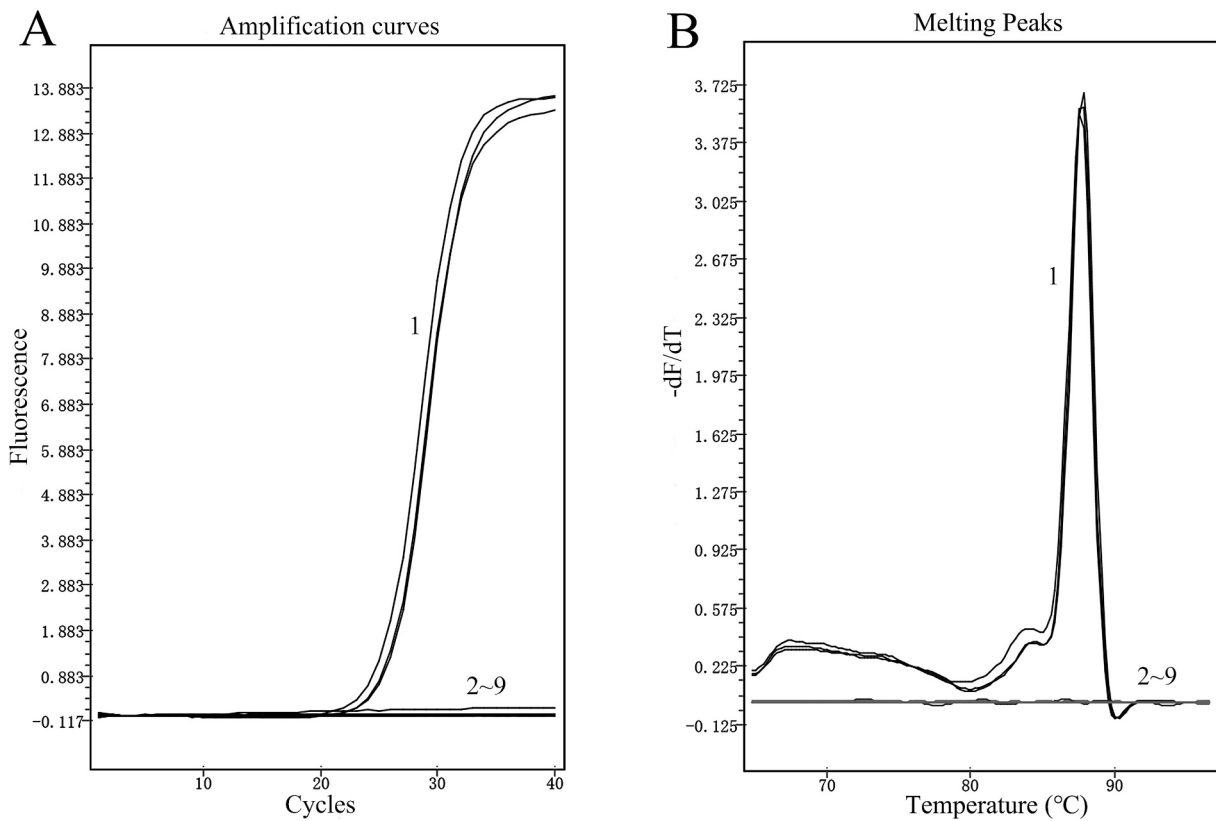


Fig. 8. Specificity analysis. A. Amplification curves; B. Melting peaks; 1: IHNV; 2~9: SHVV, GCRV, ADRV, SCRaV, SCRv, CaHV, RGV and negative control, respectively.

amplification would be severely inhibited or even terminated, while the amplification efficiency of the conventional primer was almost unaffected.

3.4. Effective annealing temperature of DPO

In order to analyze the annealing temperature effectivity of DPO

primers, IHNV cDNA was used as a template for traditional PCR (Fig. 6A). The annealing temperature ranged from 45 °C to 65 °C, and conventional primers were used as controls (Fig. 6B). DPO primers exhibited effective amplification over a wide range of annealing temperatures, with minimal impact on efficiency, while conventional primers can only be effectively amplified at several limited annealing temperatures.

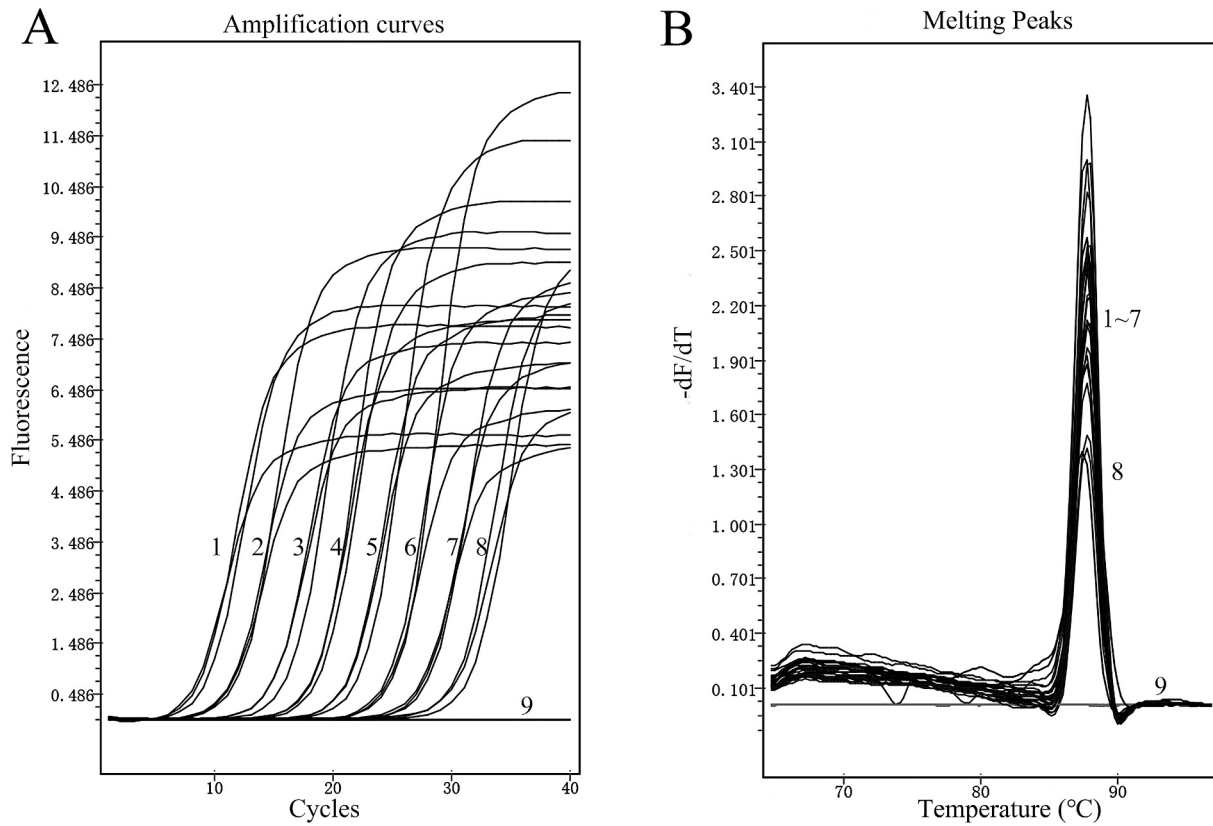


Fig. 9. The results of sensitivity test. A. Amplification curves; B. Melting peaks. 1–8: Copy number of template were 3.62×10^8 copies/ μL ~ 3.62×10^1 copies/ μL , respectively. 9: Negative control.

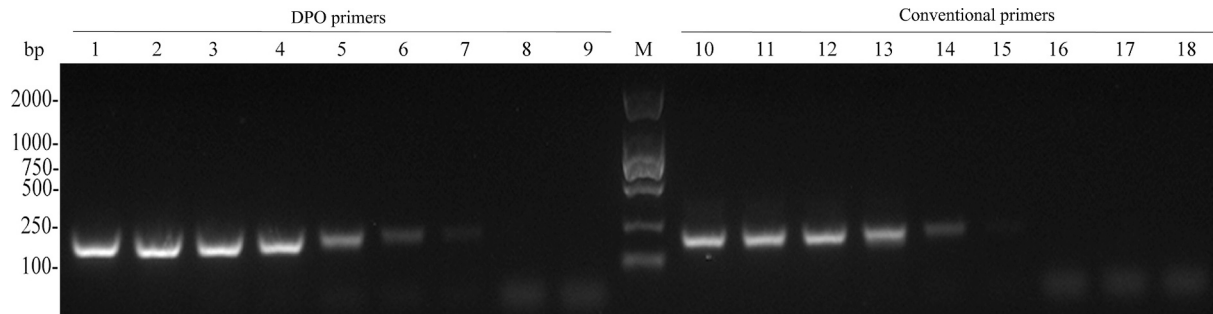


Fig. 10. Sensitivity analysis of agarose gel results by DPO primers and conventional primers. M: DL2000 DNA Marker. 1–8: Copy number of templates were 3.62×10^8 copies/ μL ~ 3.62×10^1 copies/ μL , respectively. 9 and 18: Negative controls. 1–9: DPO primers; 10–18: Conventional primers.

3.5. Standard curve establishment

Real-time PCR was carried out using DPO primers with 10-fold gradient dilutions of standard plasmid at concentrations ranging from

Table 2
Reproducibility of real-time fluorescence quantitative PCR method based on DPO primers.

Plasmid concentration (copies· μL^{-1})	Amount	Intra-assay		Inter-assay	
		Mean	CV %	Mean	CV %
3.62×10^8	3	9.05 ± 0.12	0.80	9.05 ± 0.10	0.89
3.62×10^6	3	16.68 ± 0.15	0.62	16.68 ± 0.14	0.45
3.62×10^5	3	20.16 ± 0.11	0.37	20.16 ± 0.29	0.90

3.62×10^8 to 3.62×10^4 copies/ μL as templates. The standard curve was established based on the amplification results. Linear relationships were established with lg starting quantity and Ct as the X-axis and Y-axis, respectively (Fig. 7). Finally, the standard curve equation was $Y_{\text{IHN}} = -3.954x + 40.53$, $R^2 = 0.99$.

3.6. Specificity of the DPO-based real-time PCR assay

Several aquatic animal viruses including SHVV, GCRV, SCRv, ADRV, SCRvV, CaHV and RGV were used to assess the specificity of the developed fluorescent quantitative assay developed in this study. The results showed that the amplification could only be carried out in the IHNV group, but not in any other virus groups, demonstrating excellent specificity for IHNV detection (Fig. 8).

Table 3
Clinical sample test results.

Year	n	DPO-based real-time RT-PCR		Prevalence rate IHNV	Conventional RT-PCR		Prevalence rate IHNV
		positive	negative		positive	negative	
2021	31	30	1	96.77 %	30	1	96.77 %
2022	30	26	4	86.67 %	26	4	86.67 %
2023	25	5	20	20.00 %	3	22	12.00 %
2024	23	8	15	34.78 %	7	16	30.43 %
Total	109	69	40	63.30 %	66	43	60.55 %

3.7. Sensitivity and repeatability of DPO-based real-time RT-PCR assay

The sensitivity of the method was evaluated by DPO-based real-time PCR using 10-fold diluted plasmid standard as a template. The results showed that the minimum detection limit of IHNV was 36.2 copies/ μ L (Fig. 9). Meanwhile, traditional PCR was carried out using conventional primers and DPO primers. The results showed that the minimum detection limits of DPO primers and conventional primers were 3.62×10^2 copies/ μ L and 3.62×10^3 copies/ μ L, respectively (Fig. 10). When the template concentration was 3.62×10^3 copies/ μ L, the amplification efficiency of conventional primers was still low. In general, DPO primers had higher sensitivity than conventional primers.

The repeatability results of three intra-batch and inter-batch experiments with different concentrations of plasmids were shown in Table 2. In general, the CV of IHNV was between 0.37 % and 0.90 %. All CVs were below 1 %, indicating that the DPO-based real-time PCR method established in this study had good repeatability. The coefficient of variation was calculated according to the following formula: Coefficient of Variation (CV) = (Standard Deviation (SD)/Mean) \times 100 %.

3.8. Sample testing

A total of 109 clinical samples from several trout farms were detected using the DPO-based real-time RT-PCR established in this study. The accuracy and practical applicability of the developed method were compared with those of traditional RT-PCR. As shown in Table 3, 69 IHNV positive samples were detected by fluorescence quantitative PCR based on DPO primers, with a positive rate of 63.3 %. Compared with the positive rate of 60.6 % detected by traditional RT-PCR, the DPO-based real-time RT-PCR had a higher detection rate.

4. Discussion

As living standards continue to improve, the demand for salmon and trout with high nutritional value and superior quality is increasing steadily. The aquaculture production of salmon and trout in China has been increasing. Correspondingly, effective detection and treatment of susceptible diseases (such as IHNV, IPNV, etc.) have become increasingly crucial for ensuring the health and sustainable development of salmon and trout farming.

Currently, several molecular biological detection methods for IHNV have been reported. These methods include RT-LAMP (Gunimaladevi et al., 2005), recombinase polymerase amplification (Rong et al., 2024), and RT-qPCR (Overturf and Powell, 2001; Purcell et al., 2013). These methods place high demands on primers, and the experimental conditions need to be optimized to achieve the best detection effect. Meanwhile, competitive inhibition may occur during multiplex PCR detection, resulting in a decrease of sensitivity. Based on the detection method recommended by the World Organisation for Animal Health (WOAH), nucleotide substitution in the probe region has been investigated (Hoferer et al., 2019), but the sensitivity to genotype E isolates had decreased. The study found that RT-PCR not only can be successfully applied to field investigations, but may also be slightly more sensitive than virus isolation, as a positive sample detected by RT-PCR showed a

negative result in virus isolation (Knusel et al., 2007). Moreover, RT-qPCR using N gene as the target gene can specifically distinguish North American U and M genotype IHNV isolates (Batts et al., 2022), but it is less sensitive to a particular M genotype isolate.

In recent years, the emergence of DPO primers has promoted the further development of PCR (Xu et al., 2017b; Xu et al., 2015). The DPO primers used in this study were used in conventional PCR detection. The PCR amplification was efficiently achieved when the annealing temperature was in the range of 45 °C to 65 °C, which is consistent with the results in previous studies (Li et al., 2020; Xu et al., 2017a). The non-specific amplification can be inhibited and the detection limit can be improved. Indeed, the minimum detection limit of DPO-based real-time PCR for IHNV detection established in this study can reach 36.2 copies/ μ L, which only produces specific amplification of IHNV and has no cross-reaction with other viruses. Also, since the N gene is the first gene to be transcribed in the IHNV genome and can reach high levels of transcription in the early stages of infection (Banerjee, 1987; Kurath et al., 1985; Rose and Schubert, 1987), the detection of N gene targets can theoretically reach a lower detection limit.

At present, IHNV is mainly divided into five genotypes: U, M, L, E and J genotypes (Jia et al., 2017; Nishizawa et al., 2006). Genotype J was considered as the main epidemic strain in China (Xu et al., 2019a), but the M (Jia et al., 2018) and U (Huo et al., 2022) genotypes were also detected in some areas. The fluorescence quantitative PCR detection method based on DPO primers can quickly detect IHNV qualitatively and quantitatively. However, amplification reactions will not proceed when the template has more than three site mutations. In this study, the conservation analysis of multiple IHNV strains was carried out when designing DPO primers. Referring to the previous method (Lee et al., 2008), the bases targeting the variable nucleotide sites in viral genomes were replaced with deoxyinosine in the central region of the DPO primers. This makes it theoretically possible to achieve better detection efficiency when detecting IHNV strains of different genotypes. Moreover, this also gives us some inspiration. If the 3'-segment of the DPO primer targets the highly mutable site in the viral genome, the amplification efficiency may vary among strains during detection, which may enable accurate strain typing.

Besides IHNV, IPNV is also an important pathogen in salmonid-susceptible diseases, and they are often co-infected (Vilas et al., 1994). The method established in this study has great advantages for the accurate detection of IHNV in co-infected samples or complex samples. Additionally, it may also lay a foundation for the further establishment of multiplex RT-qPCR detection methods.

In conclusion, the DPO primer-based real-time fluorescent RT-PCR method developed in this study provides rapid, accurate detection of IHNV, demonstrating high specificity and sensitivity. Importantly, both the 5'-segment and 3'-segment of the DPO primers used in this study are located in the conserved regions of the N gene, and the non-conserved region in the middle is linked by deoxyinosine. Therefore, this detection method can detect almost all IHNV isolates, which can be used for epidemiological monitoring or as part of diagnostic methods. Furthermore, this study lays a foundation for the development of similar detection methods for other aquatic animal viruses, offering a valuable tool for both epidemiological monitoring and diagnostic purposes.

CRedit authorship contribution statement

Shihao Zheng: Writing – original draft, Visualization, Validation, Investigation, Data curation. **Jingwen Huang:** Validation, Investigation, Data curation. **Qiuji Li:** Validation, Investigation, Data curation. **Xinyue Zhou:** Validation, Investigation, Data curation. **Yutong Yang:** Validation, Investigation, Data curation. **Hongying Zhao:** Validation, Investigation, Data curation. **Wenlong Zhang:** Project administration, Funding acquisition. **Yongsheng Cao:** Writing – review & editing, Visualization, Validation, Project administration, Methodology, Data curation, Conceptualization.

Declaration of competing interest

The authors declare no conflict of interest.

Acknowledgements

We thank Professor Jiagang Tu (Huazhong Agricultural University) and Fei Ke (Institute of Hydrobiology, Chinese Academy of Sciences) for contributing the nucleic acids of aquatic animal viruses, which facilitated the specificity test. This work was supported by National Natural Science Foundation of China to Y. C. (Grant No. 32273178), Heilongjiang Provincial Natural Science Foundation to Y. C. (Grant No. YQ2022C020) and to W. Z. (Grant No. ZL2024C019), and “Basic Research Support Programme for Outstanding Young Teachers in Heilongjiang Province” to W. Z. (Grant No. YQJH2023184).

Data availability

Data will be made available on request.

References

- Abbadì, M., Gastaldelli, M., Pascoli, F., Zamperin, G., Buratin, A., Bedendo, G., Toffan, A., Panzarin, V., 2021. Increased virulence of Italian infectious hematopoietic necrosis virus (IHN) associated with the emergence of new strains. *Virus Evol.* 7 (2), veab056.
- Arnzen, J.M., Ristow, S.S., Hesson, C.P., Lientz, J., 1991. Rapid fluorescent antibody tests for infectious Hematopoietic necrosis virus (IHN) utilizing monoclonal antibodies to the nucleoprotein and glycoprotein. *J. Aquat. Anim. Health* 3 (2), 109–113.
- Banerjee, A.K., 1987. Transcription and replication of rhabdoviruses. *Microbiol. Rev.* 51 (1), 66–87.
- Batts, W.N., Capps, T.R., Crosson, L.M., Powers, R.L., Breyta, R., Purcell, M.K., 2022. Rapid diagnostic test to detect and discriminate infectious hematopoietic necrosis virus (IHN) genogroups U and M to aid management of Pacific Northwest Salmonid populations. *Animals* 12 (14), 1761.
- Bei, C., Zhang, C., Wu, H., Feng, H., Zhang, Y.-A., Tu, J., 2023. DDX3X is hijacked by snakehead Vesiculovirus phosphoprotein to facilitate virus replication via stabilization of the phosphoprotein. *J. Virol.* 97 (2), e00035–23.
- Carrara, L., Navarro, F., Turbau, M., Seres, M., Moran, I., Quintana, I., Martino, R., Gonzalez, Y., Brell, A., Cordon, O., Diestra, K., Mata, C., Mirelis, B., Coll, P., 2013. Molecular diagnosis of bloodstream infections with a new dual-priming oligonucleotide-based multiplex PCR assay. *J. Med. Microbiol.* 62 (11), 1673–1679.
- Chamberlain, J.S., Gibbs, R.A., Ranier, J.E., Nguyen, P.N., Caskey, C.T., 1988. Deletion screening of the Duchenne muscular dystrophy locus via multiplex DNA amplification. *Nucleic Acids Res.* 16 (23), 11141–11156.
- Chun, J.Y., Kim, K.J., Hwang, I.T., Kim, Y.J., Lee, D.H., Lee, I.K., Kim, J.K., 2007. Dual priming oligonucleotide system for the multiplex detection of respiratory viruses and SNP genotyping of CYP2C19 gene. *Nucleic Acids Res.* 35 (6), e40.
- Chung, W.C., Jung, S.H., Oh, J.H., Kim, T.H., Cheung, D.Y., Kim, B.W., Kim, S.S., Kim, J. I., Sin, E.Y., 2014. Dual-priming oligonucleotide-based multiplex PCR using tissue samples in rapid urease test in the detection of *Helicobacter pylori* infection. *World J. Gastroenterol.* 20 (21), 6547–6553.
- Dhar, A.K., Bowers, R.M., Licon, K.S., Lapatra, S.E., 2008. Detection and quantification of infectious hematopoietic necrosis virus in rainbow trout (*Oncorhynchus mykiss*) by SYBR green real-time reverse transcriptase-polymerase chain reaction. *J. Virol. Methods* 147 (1), 157–166.
- Garver, K.A., Mahony, A.A., Stucchi, D., Richard, J., Van Woensel, C., Foreman, M., 2013. Estimation of parameters influencing waterborne transmission of infectious hematopoietic necrosis virus (IHN) in Atlantic salmon (*Salmo salar*). *PLoS ONE* 8 (12), e82296.
- Gunimaladevi, I., Kono, T., Lapatra, S.E., Sakai, M., 2005. A loop mediated isothermal amplification (LAMP) method for detection of infectious hematopoietic necrosis virus (IHN) in rainbow trout (*Oncorhynchus mykiss*). *Arch. Virol.* 150 (5), 899–909.
- Hoferer, M., Akimkin, V., Skrypski, J., Schutze, H., Sting, R., 2019. Improvement of a diagnostic procedure in surveillance of the listed fish diseases IHN and VHS. *J. Fish Dis.* 42 (4), 559–572.
- Huang, J., Zheng, S., Li, Q., Zhao, H., Zhou, X., Yang, Y., Zhang, W., Cao, Y., 2024. Host miR-146a-3p facilitates replication of infectious hematopoietic necrosis virus by targeting WNT3a and CCND1. *Vet. Sci.* 11 (5), 204.
- Huo, C., Ma, Z., Li, F., Xu, F., Li, T., Zhang, Y., Jiang, N., Xing, W., Xu, G., Luo, L., Sun, H., 2022. First isolation and pathogenicity analysis of a genogroup U strain of infectious hematopoietic necrosis virus from rainbow trout in China. *Transbound. Emerg. Dis.* 69 (2), 337–348.
- Jia, P., Purcell, M.K., Pan, G., Wang, J., Kan, S., Liu, Y., Zheng, X., Shi, X., He, J., Yu, L., Hua, Q., Lu, T., Lan, W., Winton, J.R., Jin, N., Liu, H., 2017. Analytical validation of a reverse transcriptase droplet digital PCR (RT-ddPCR) for quantitative detection of infectious hematopoietic necrosis virus. *J. Virol. Methods* 245, 73–80.
- Jia, P., Breyta, R.B., Li, Q., Qian, X., Wu, B., Zheng, W., Wen, Z., Liu, Y., Kurath, G., Hua, Q., Jin, N., Liu, H., 2018. Insight into infectious hematopoietic necrosis virus (IHN) in Chinese rainbow trout aquaculture from virus isolated from 7 provinces in 2010–2014. *Aquaculture* 496, 239–246.
- Ke, F., Gui, J.-F., Chen, Z.-Y., Li, T., Lei, C.-K., Wang, Z.-H., Zhang, Q.-Y., 2018. Divergent transcriptomic responses underlying the ranaviruses-amphibian interaction processes on interspecies infection of Chinese giant salamander. *BMC Genomics* 19, 211.
- Ke, F., Meng, X.-Y., Zhang, Q.-Y., 2022. *Siniperca chuatsi* Rhabdovirus (SCRV)-induced key pathways and major antiviral genes in fish cells. *Microorganisms* 10 (12), 2464.
- Knusel, R., Bergmann, S.M., Einer-Jensen, K., Casey, J., Segner, H., Wahli, T., 2007. Virus isolation vs RT-PCR: which method is more successful in detecting VHSV and IHNV in fish tissue sampled under field conditions? *J. Fish Dis.* 30 (9), 559–568.
- Kolodziejek, J., Schachner, O., Durrwald, R., Latif, M., Nowotny, N., 2008. “mid-G” region sequences of the glycoprotein gene of Austrian infectious hematopoietic necrosis virus isolates form two lineages within European isolates and are distinct from American and Asian lineages. *J. Clin. Microbiol.* 46 (1), 22–30.
- Kurath, G., Ahern, K.G., Pearson, G.D., Leong, J.C., 1985. Molecular cloning of the six mRNA species of infectious hematopoietic necrosis virus, a fish rhabdovirus, and gene order determination by R-loop mapping. *J. Virol.* 53 (2), 469–476.
- Kurath, G., Winton, J.R., Dale, O.B., Purcell, M.K., Falk, K., Busch, R.A., 2016. Atlantic salmon, *Salmo salar* L. are broadly susceptible to isolates representing the north American genogroups of infectious hematopoietic necrosis virus. *J. Fish Dis.* 39 (1), 55–67.
- Lapatra, S.E., Roberti, K.A., Rohovec, J.S., Fryer, J.L., 1989. Fluorescent antibody test for the rapid diagnosis of infectious hematopoietic necrosis. *J. Aquat. Anim. Health* 1 (1), 29–36.
- Lee, C.S., Kang, B.K., Lee, D.H., Lyoo, S.H., Park, B.K., Ann, S.K., Jung, K., Song, D.S., 2008. One-step multiplex RT-PCR for detection and subtyping of swine influenza H1, H3, N1, N2 viruses in clinical samples using a dual priming oligonucleotide (DPO) system. *J. Virol. Methods* 151 (1), 30–34.
- Li, D.D., Hao, C.B., Liu, Z.M., Wang, S.J., Wang, Y., Chao, Z., Gao, S.Y., Chen, S., 2020. Development of a novel dual priming oligonucleotide system-based PCR assay for specific detection of *Salmonella* from food samples. *J. Food Saf.* 40 (3), e12789.
- Medina, D.J., Chang, P.W., Bradley, T.M., Yeh, M.T., Sadasiv, E.C., 1992. Diagnosis of infectious hematopoietic necrosis virus in Atlantic salmon *Salmo salar* by enzyme-linked immunosorbent assay. *Dis. Aquat. Org.* 13, 147–150.
- Mulei, I.R., Nyaga, P.N., Muthia, P.G., Waruiru, R.M., Xu, C., Evensen, O., Mutoloki, S., 2019. First detection and isolation of infectious haematopoietic necrosis virus from farmed rainbow trout in Nyeri County, Kenya. *J. Fish Dis.* 42 (5), 751–758.
- Nishizawa, T., Kinoshita, S., Kim, W., Higashi, S., Yoshimizu, M., 2006. Nucleotide diversity of Japanese isolates of infectious hematopoietic necrosis virus (IHN) based on the glycoprotein gene. *Dis. Aquat. Org.* 71, 267–272.
- Overturf, K.S.E.L., Powell, M., 2001. Real-time PCR for the detection and quantitative analysis of IHNV in salmonids. *J. Fish Dis.* 24 (6), 325–333.
- Pan, Y., Liu, Z., Quan, J., Gu, W., Wang, J., Zhao, G., Lu, J., Wang, J., 2024. Purified *Astragalus polysaccharide* combined with inactivated vaccine markedly prevents infectious Hematopoietic necrosis virus infection in rainbow trout (*Oncorhynchus mykiss*). *ACS Biomater. Sci. Eng.* 10 (11), 6938–6953.
- Pei, C., Ke, F., Chen, Z.-Y., Zhang, Q.-Y., 2014. Complete genome sequence and comparative analysis of grass carp reovirus strain 109 (GCRV-109) with other grass carp reovirus strains reveals no significant correlation with regional distribution. *Arch. Virol.* 159, 2435–2440.
- Purcell, M.K., Thompson, R.L., Garver, K.A., Hawley, L.M., Batts, W.N., Sprague, L., Sampson, C., Winton, J.R., 2013. Universal reverse-transcriptase real-time PCR for infectious hematopoietic necrosis virus (IHN). *Dis. Aquat. Org.* 106 (2), 103–115.
- Rong, F., Wang, H., Tang, X., Xing, J., Sheng, X., Chi, H., Zhan, W., 2024. The development of RT-RPA and CRISPR-Cas12a based assay for sensitive detection of infectious hematopoietic necrosis virus (IHN). *J. Virol. Methods* 326, 114892.
- Rose, J., Schubert, M., 1987. Rhabdovirus genomes and their products. In: Wagner, R.R. (Ed.), *The Rhabdoviruses*. Springer, US, pp. 129–166.
- Rucker, R.R., Whipple, W.J., Parvin, J.R., Evans, C.A., 1953. A contagious disease of salmon, possibly of virus origin. *Fish B-Noaa* 54 (1), 35–46.
- See, S.A., Goh, Z.H., Chan, Y.Y., Chong, K.E., Tan, G.Y.A., Bhassu, S., Othman, R.Y., 2021. Biosafety evaluation and detection of shrimp viruses on field samples using dual priming oligonucleotide (DPO) system based multiplex PCR assay. *Gene Rep.* 23, 101158.
- Shao, Y., Zhao, J., Ren, G., Lu, T., Chen, X., Xu, L., 2022a. Early or simultaneous infection with infectious pancreatic necrosis virus inhibits infectious hematopoietic necrosis virus replication and induces a stronger antiviral response during co-infection in rainbow trout (*Oncorhynchus mykiss*). *Viruses* 14 (8), 1732.

- Shao, Y., Zhao, J., Ren, G., Lu, T., Xu, L., 2022b. Infectious hematopoietic necrosis virus promoted infectious pancreatic necrosis virus multiplication during co-infection in rainbow trout (*Oncorhynchus mykiss*). *Aquaculture* 561, 738649.
- Vilas, M.P., Rodríguez, S., Pérez, S., 1994. A case of coinfection of IPN and IHN virus in farmed rainbow trout in Spain. *B Eur. Assoc. Fish Pat.* 14, 47–50.
- Walker, P.J., Freitas-Astúa, J., Bejerman, N., Blasdel, K.R., Breyta, R., Dietzgen, R.G., Fooks, A.R., Kondo, H., Kurath, G., Kuzmin, I.V., Ramos-González, P.L., Shi, M., Stone, D.M., Tesh, R.B., Tordo, N., Vasilakis, N., Whitfield, A.E., 2022. ICTV virus taxonomy profile: Rhabdoviridae 2022. *J. Gen. Virol.* 103 (6), 001689.
- Williams, K., Blake, S., Sweeney, A., Singer, J.T., Nicholson, B.L., 1999. Multiplex reverse transcriptase PCR assay for simultaneous detection of three fish viruses. *J. Clin. Microbiol.* 37 (12), 4139–4141.
- Xu, Y.G., Liu, Z.M., Guan, X.T., Cui, L.C., Li, S.L., 2015. Dual priming oligonucleotide (DPO)-based multiplex PCR assay for specific detection of four diarrhoeagenic *Escherichia coli* in food. *Lett. Appl. Microbiol.* 61 (2), 146–152.
- Xu, Y.-G., Sun, B., Zhao, H.-Y., Liu, Z.-M., Jiang, Y.-P., Wang, L., Qiao, X.-Y., Li, Y.-J., Tang, L.-J., 2017a. Development and evaluation of a dual priming oligonucleotide system-based multiplex PCR assay for simultaneous detection of six foodborne pathogens. *Eur. Food Res. Technol.* 243 (4), 555–563.
- Xu, Y.-G., Sun, L.-M., Wang, Y.-S., Chen, P.-P., Liu, Z.-M., Li, Y.-J., Tang, L.-J., 2017b. Simultaneous detection of *Vibrio cholerae*, *Vibrio alginolyticus*, *Vibrio parahaemolyticus* and *Vibrio vulnificus* in seafood using dual priming oligonucleotide (DPO) system-based multiplex PCR assay. *Food Control* 71, 64–70.
- Xu, L., Zhao, J., Liu, M., Kurath, G., Breyta, R.B., Ren, G., Yin, J., Liu, H., Lu, T., 2019a. Phylogeography and evolution of infectious hematopoietic necrosis virus in China. *Mol. Phylogenet. Evol.* 131, 19–28.
- Xu, L., Zhao, J., Ren, G., Ying, D., Lin, J., Cao, Y., Yin, J., Liu, H., Lu, T., Zhang, Q., 2019b. Co-infection of infectious hematopoietic necrosis virus (IHN) and infectious pancreatic necrosis virus (IPNV) caused high mortality in farmed rainbow trout (*Oncorhynchus mykiss*) in China. *Aquaculture* 512, 734286.
- Yeh, J.Y., Lee, J.H., Seo, H.J., Park, J.Y., Moon, J.S., Cho, I.S., Choi, I.S., Park, S.Y., Song, C.S., Lee, J.B., 2011. Simultaneous detection of Rift Valley fever, bluetongue, rinderpest, and Peste des petits ruminants viruses by a single-tube multiplex reverse transcriptase-PCR assay using a dual-priming oligonucleotide system. *J. Clin. Microbiol.* 49 (4), 1389–1394.
- Yu, X.-D., Ke, F., Zhang, Q.-Y., Gui, J.-F., 2023. Genome characteristics of two ranavirus isolates from mandarin fish and largemouth bass. *Pathogens* 12 (5), 730.